Micellization of Model Graft Copolymers of the H and π Type in Dilute Solution

Stergios Pispas[†] and Nikos Hadjichristidis*[,†]

Department of Chemistry, University of Athens, Panepistimiopolis, Zografou, 157 71 Athens, Greece

Jimmy W. Mays

Department of Chemistry, University of Alabama at Birmingham, Birmingham, Alabama 35294

Received March 28, 1996; Revised Manuscript Received August 28, 1996[⊗]

ABSTRACT: The dilute solution properties of model graft copolymers of the H, S_2IS_2, and π type, (S,I)I-(I,S), have been studied in common good (THF) and selective (*n*-decane and ethyl acetate) solvents. The molecules have two trifunctional branch points and are composed of polyisoprene (PI) bridges and polystyrene (PS) or polyisoprene branches. Three different methods were employed, low-angle laser light scattering, dynamic light scattering, and viscometry, in order to extract information about the aggregation number, the size, and the shape of the micelles formed in selective solvents for the PI backbones (*n*-decane) and for the PS branches (ethyl acetate). Both graft copolymers form multimolecular micelles in *n*-decane. Their hydrodynamic behavior resembles that of hard spheres. In the case of the H copolymer in ethyl acetate, large, loosely bound aggregates are formed above the cmc which are transformed to more compact micelles at higher concentrations. For the π copolymer, regions of existence of unimolecular and compact multimolecular micelles were observed, together with a sharp and relatively high critical micelle concentration. The behavior is in agreement with the closed association model. In both cases, the aggregation numbers were lower than the ones observed for diblock and triblock copolymers in similar solvents. The influence of macromolecular architecture on the micellization behavior of these model compounds is discussed in view of the additional constraints and parameters imposed by the macromolecular topology.

Introduction

Macromolecular association has been the subject of many studies for more than 30 years[1] now, since aggregating systems are of great academic interest (structure−property relations) and have potential for applications in fluids science (i.e. viscosity modifiers).[2] In addition, it has long been recognized that the structure of polymer solutions can influence the properties of the final solid polymeric product.[3]

It is a well-established fact that block copolymers form micelles in selective solvents.[4] i.e. solvents that are good for one of the blocks and precipitants for the other. Experimental parameters such as molecular weight of the copolymer or of each block, composition and architecture of the copolymer as a whole, solvent quality with respect to both blocks, concentration, and temperature can dramatically influence the aggregation number, the size, and the shape of the micelles formed. So far, most of the investigations have been concerned with the micellization of linear diblock copolymers.[5−15] Experimental and theoretical studies dealing with the ability of triblock copolymers to form micelles in selective solvents for the middle or the outer blocks have also been published.[16−27] A few papers dealing with graft copolymers, having randomly distributed branches along the backbone,[28−32] and a limited number of papers dealing with more complex architectures (star and super-H) have also appeared in the literature.[33−36] More investigations on nonlinear block copolymers are needed in order to elucidate the influence of the architecture on the micellization behavior of block copolymers.

Scheme 1

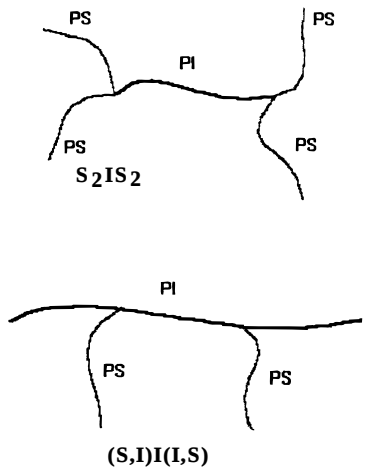

In this paper, we report results from low-angle laser light scattering, dynamic light scattering, and viscometry experiments on two well-characterized model graft copolymers of the H, S_2IS_2 and π (S,I)I(I,S) architectures (Scheme 1) in dilute solutions of selective solvents for the polyisoprene backbones (*n*-decane) and the polystyrene branches (ethyl acetate). Our primary goal is to investigate the influence of the macromolecular topology on fundamental properties of the micelles (aggregation number, size, and shape) and compare their behavior with the behavior of micelles formed by linear diblock and triblock copolymers.

Experimental Section

A. Polymer Synthesis. Both model macromolecules were synthesized by anionic polymerization high-vacuum techniques,[37] using methyltrichlorosilane as linking agent. The

[†] Also at the Institute of Electronic Structure and Laser, FORTH, 711 10 Heraklion, Crete, Greece.

[⊗] Abstract published in *Advance ACS Abstracts,* October 1, 1996.

S0024-9297(96)00474-3 CCC: $12.00

Scheme 2

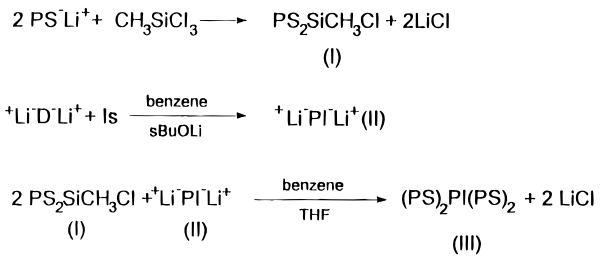

Scheme 3

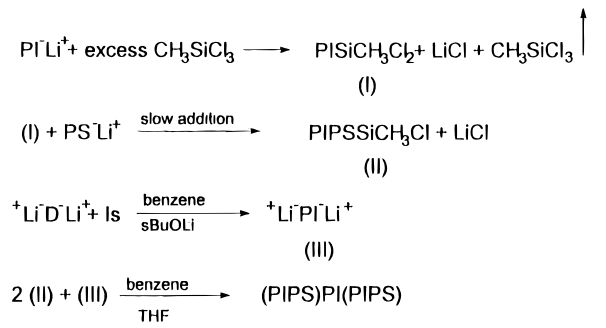

difunctional initiator derived from 1,3-bis(1-phenylethenyl)-benzene (PEB) in nonpolar solvent (benzene) was used for the preparation of the connecting parts of the backbones, ensuring uniformity in polyisoprene microstructure (ca. 92% 1,4, ca. 8% 3,4). The reactions describing the synthesis of the H copolymer, S_2IS_2, are shown in Scheme 2.

The synthetic route involves the reaction of living poly(styryllithium) with CH_3SiCl_3 in an 2.1:3 Li/Cl ratio. After the formation of the difunctional living polyisoprene bridge, by use of the difunctional initiator, and its end-capping with the centrally functional PS dimer, the H copolymer is formed. The desired product was separated from the excess arms by fractionation in a toluene/methanol mixture.

The synthesis of the π-shaped copolymer, (S,I)I(I,S), with a PI backbone and two equally spaced PS branches is decribed in Scheme 3.

In this case, the outer PI part of the backbone is formed first by reaction of living monofunctional PILi with excess CH_3SiCl_3. After the removal of excess CH_3SiCl_3, on the vacuum line, the PS branch was added slowly until complete substitution of the second chlorine atom on the macromolecular difunctional PI linking agent. The PS−PI diblock thus formed, having a reactive Cl at the junction point, was reacted with the difunctional living PI bridge in a 2.2:1 ratio. The π-shaped copolymer was isolated after fractionation in toluene/methanol mixture. The molecular characteristics of the graft copolymers are shown in Table 1. More details concerning the sample synthesis are given elsewhere.[38]

B. Solvent Purification and Solution Preparation. Analytical grade THF was refluxed over sodium for 24 h and fractionally distilled just prior to use. Both copolymers are readily dissolved in this solvent at room temperature since this is a good solvent for both blocks. Solutions for static low-angle light scattering measurements were prepared by dilution of a stock solution and were filtered through 0.22 μm Nylon filters directly into the scattering cell. For the dynamic light scattering measurements and static light scattering measurements at temperatures above ambient, clarification of the solutions was accomplished through a closed-loop filtration system. Dilutions were made in the filtering assembly in this case. For the viscosity measurements 1.2 μm Nylon filters were used and dilutions were made directly into the viscometer. The same dilution methods were applied for the solutions made with the selective solvents. However, 0.45 μm and 1.2 or 5 μm Nylon filters were used for the light scattering and the viscosity experiments, respectively, on the micellar solutions.

n-Decane (analytical grade) was dried over CaH_2 by refluxing for at least 24 h and was fractionally distilled just before use. The π-shaped copolymer was completely soluble in *n*-decane after standing for 24 h, with occasional shaking of the stock solutions. As a precaution, a final heating at 60 °C for 2 h was done before dilutions in order to avoid sample history effects related to the formation of nonequilibrium structures in solution. For the dissolution of the H-shaped copolymer, heating of the stock solutions at 60 °C overnight was necessary, apparently due to the higher PS content. Both polymers gave solutions having the characteristic bluish tint due to the presence of micelles. No precipitation was observed from these solutions after standing at room temperature for weeks.

Table 1. Molecular Characteristics of Model Graft Copolymers in THF

sample	S_2IS_2 (H polymers)	(S,I)I(I,S) (π polymers)
$M_w \times 10^{-5}$ [a]	1.74	1.47
$M_n \times 10^{-5}$ [b]	1.71	1.33
M_w/M_n [c]	1.08	1.09
wt % PS [d]	42	24
M_n(PS arm) $\times 10^{-4}$ [b]	2.03	1.91
M_n (PI arm) $\times 10^{-4}$ [b]		3.72
M_n (PI bridge) $\times 10^{-4}$ [b]	10.2	3.33
$[\eta]$ (mL/g)	101	85.3
k_H	0.39	0.41
R_v (nm)	14.1	12.6
D_0 (cm^2/s) $\times 10^7$	3.88	4.34
k_D	58	44
R_h (nm)	12.2	11.0
R_v/R_h	1.16	1.15

[a] Low-angle laser light scattering. [b] Membrane osmometry in toluene at 37 °C. [c] Size exclusion chromatography. [d] UV spectroscopy at 260 nm.

Ethyl acetate (analytical grade) was stirred over potassium carbonate for 48 h and subsequently over phosphorus pentoxide for another 24 h. The solvent was fractionally distilled just before use. The H copolymer was readily soluble at room temperature, and although this temperature is higher than the PI's T_g of −65 °C(∼90 deg higher), a subsequent heating at 45 °C was carried out. The stock solutions had the bluish color of micellar solutions and were stable for weeks. The π copolymer was insoluble at room temperature, probably due to the low PS content. It could be solubilized (at concentrations of 1−2% w/v) after heating at 45 °C for 2 h maximum, giving clear transparent solutions. By cooling, a cloud point was observed at around 37 °C for 1−2% w/v solutions. At ∼36 °C, the stock solutions became "milky", making light scattering experiments impossible. Further standing at room temperature resulted in precipitation of the polymer. These heating−cooling cycles could be repeated with reproducibility many times. At last, it was decided to study this sample at 40 °C. Ethyl acetate is still a precipitant for PI at this temperature, as solubility experiments on a 75 000 molecular weight PI homopolymer indicated. This homopolymer is insoluble in ethyl acetate at 45 °C even after several days, and dissolution is achieved only after standing for several hours at 55 °C. We feel that this solvent−temperature combination is sufficient to study the micellization properties of the π-shaped copolymer. In addition, the solution preparation protocol outlined above, for both selective solvents, ensured reproducibility and consistency of the experimental results.

C. Methods. Static light scattering measurements were performed with a Chromatix KMX-6 low-angle laser light scattering photometer, equipped with a 2 mW He−Ne laser, operating at $\lambda = 633$ nm. At temperatures above ambient, a laboratory-built temperature control system was used. Apparent weight-average molecular weights, $M_{w,app}$, and second virial coefficients, A_2, were determined from the concentration dependence of the reduced scattering intensity by use of the equation

$$Kc/\Delta R_\theta = 1/M_{w,\,app} + 2A_2c + \ldots \quad (1)$$

where K is a combination of optical and physical constants,

including the differential refractive index increment, dn/dc, c is the concentration, and ΔR_θ is the difference between the Rayleigh ratio of the solution and the solvent. The dn/dc values required for the light scattering measurements were obtained by a Chromatix KMX-16 laser differential refractometer, operating at 633 nm and calibrated with NaCl solutions, in the appropriate solvent and temperature.

Dynamic light scattering experiments were carried out on a Brookhaven system composed of a BI200SM goniometer, a BI2030AT correlator with 72 channels, a ca. 28 mW Ar+ laser operating at $\lambda = 488$ nm, and a thermostated bath (temperature stability ±0.1 °C). The temperature control of the closed-loop system was achieved by the aid of the same unit used in high-temperature static light scattering measurements. The scattering intensity was measured at forward scattering angles between 37.5 and 90°. Correlation functions were analyzed, to second order, by the method of cumulants. Apparent translational diffusion coefficients at zero concentration, $D_{0,app}$, were calculated, after extrapolation at zero angle, by aid of the equation

$$D_{app} = D_{0,app}(1 + k_D c + ...) \quad (2)$$

where D_{app} is the apparent diffusion coefficient at each concentration at zero angle and k_D is the coefficient of the concentration dependence of D_{app}. Appparent hydrodynamic radii, R_h,were determined using the equation

$$R_h = k_B T/6\pi\eta_o D_{0,app} \quad (3)$$

where k_B is the Boltzmann constant, T is the absolute temperature, and η_o is the viscosity of the solvent.

For the viscosity measurements, Cannon-Ubbelohde dilution viscometers were used in a temperature-controlled bath (temperature stability ±0.02 °C). Flow times were measured with a Schott-Geräte automatic flow timer and were always greater than 150 s. Kinetic energy corrections were made for the lower flow times (less than 200 s). Data were analyzed by using the Huggins

$$\eta_{sp}/c = [\eta] + k_H[\eta]^2 c + ... \quad (4)$$

and Kraemer

$$\ln \eta_r/c = [\eta] + k_K[\eta]^2 c + ... \quad (5)$$

equations, where $[\eta]$ is the intrinsic viscosity and k_H and k_K are the Huggins and Kraemer constants, respectively. Viscometric radii, R_v, were calculated via the equation

$$R_v = (3/10\pi N_A)^{1/3}(M_{w,app}[\eta])^{1/3} \quad (6)$$

where N_A is the Avogadro number and $M_{w,app}$ is the molecular weight determined by static light scattering. In all cases, measurements were extended over the largest accessible concentration range, defined by instrumental accuracy.

Results and Discussion

A. Hydrodynamic Properties in THF. From the molecular weight and compositional characterization of the model graft copolymers, it is evident that the samples possess high degrees of molecular weight and compositional homogeneity. The hydrodynamic properties of the model graft copolymers in THF, a good solvent for both PS and PI segments, are also listed in Table 1. The experimental k_H values are typical of flexible polymeric chains in good solvents and close to the theoretical good solvent limit, $k_H \sim 1/3$, for flexible homopolymers. Additionally, the R_v/R_h ratio is equal to 1.16 and 1.15 for the H and π copolymers, respectively, somewhat higher than the the theoretical limit for rigid spheres ($R_v/R_h = 1.0$[39]), but lies in the upper range of experimentally determined values for linear homopolymers in good solvents.[40−46] It has to be kept in mind that the ratio R_v/R_h may reflect changes in the shape of the polymer coil since the intrinsic viscosity contains static and dynamic contributions ($[\eta] \propto R_h R_G^2$), where R_h is a purely hydrodynamic quantity. Additionally, in copolymers comprised of incompatible segments, partial segregation on the molecular level may influence to a greater extent the static properties of the molecule. Conclusions about the shape of the effective hydrodynamic ellipsoid, describing the hydrodynamic behavior of the samples in THF, can be deduced by using the Mandelkern−Flory−Scheraga[47] parameter, β_{MFS}, defined by the equation

$$\beta_{MFS} = (D\eta_o/k_B T)(M[\eta])^{1/3} \quad (7)$$

in a more quantitative fashion. β_{MFS} depends strongly on the $p = a/b$ axis ratio for prolate ellipsoids (a is the major semiaxis and b the minor semiaxis), while for oblate ellipsoids, β_{MFS} is almost independent of the axis ratio. The ratio has the values of 2.12×10^6 and 2.19×10^6 for spheres ($p = 1$) and random coils, respectively. For prolate ellipsoids with $p = 20$, $\beta_{MFS} = 2.64 \times 10^6$. The β_{MFS} values for the H and π copolymers are equal to 2.43×10^6 for both samples, considerably larger than the hard sphere and random coil values, indicating a more elongated shape for these macromolecules.

Table 2. Micellar Properties of Model Graft Copolymers in *n*-Decane at 25 °C

sample	$M_{w,app} \times 10^{-6}$	$A_2 \times 10^6$	N_w[a]	$[\eta]$ (mL/g)	k_H	R_v (nm)	$D_{0,app}$ (cm^2/s) $\times 10^8$	k_D	R_h (nm)	R_v/R_h
S_2IS_2	14	7.5	80	58.4	0.93	50.6	5.38	94	47.1	1.08
(S,I)I(I,S)	1.81	6.2	12	44.8	1.15	23.4	10.7	60	23.7	0.99

[a] Degree of association $N_w = (M_{w,app})/(M_{w,copol}$ in THF).

B. Micellar Properties in *n*-Decane. The results from the experiments in n-decane, a selective solvent for the PI segments, are given in Table 2. The concentration dependence of the reduced scattering intensity is a classical example of systems presenting association[48] (Figure 1). The $Kc/\Delta R_\theta$ values, after a very steep decrease at lower concentrations, show an upturn with a positive slope. This indicates that in this high-concentration region the equilibrium is shifted in favor of the micelles and the properties of the solution are dominated by the presence of associates made of several copolymer chains. However, even for the lower concentrations studied, the region of molecularly dissolved unimers was never reached and no cmc (critical micelle concentration) was detected for either sample, indicating that its value must be very low (lower than 8×10^{-6} g/mL for the H copolymer and $<4 \times 10^{-5}$ g/mL for the π copolymer), in accordance with previous observations on similar systems. Judging from the occurrence of the inflection point on the curves and the lower aggregation number for the π copolymer, one would expect that the cmc value for this sample would be larger than for the H copolymer. The apparent weight-average molecular weights determined by linear extrapolation from high concentrations are considerably larger than the ones determined for the isolated molecules in THF, and the values of the second virial coefficients are extremely small but positive. Due to the high dn/dc value for these samples in n-decane (0.141 and 0.134 mL g^{-1} for the H and π, respectively), their low degree of heterogeneity, and the low A_2 values, the experimental $M_{w,app}$ values must be very close to the true ones. Definitely these samples form multimolecular micelles in n-decane, with

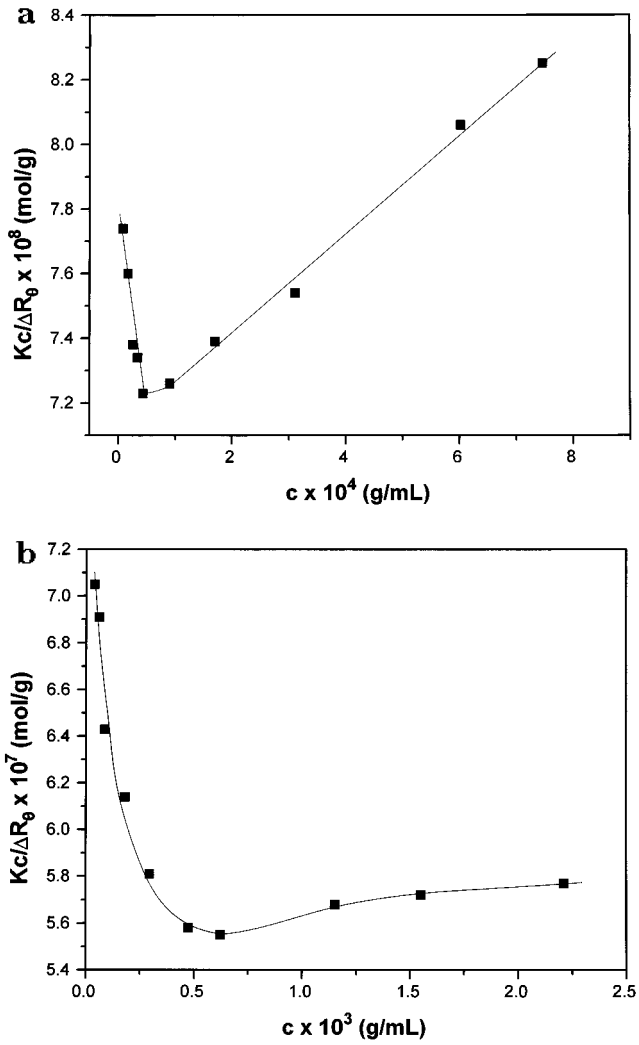

Figure 1. Static light scattering plots for (a) sample S_2IS_2 (top) and (b) sample (S,I)I(I,S) (bottom) in *n*-decane at 25 °C ($\theta = 4.6°$).

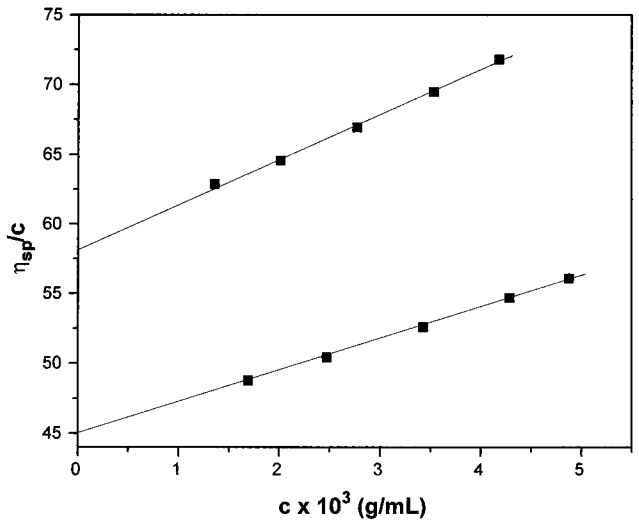

Figure 2. Viscosity plots for sample S_2IS_2 (top) and sample (S,I)I(I,S) (bottom) in *n*-decane at 25 °C.

the weight-average aggregation number being larger for the H copolymer, which also contains more PS.

Viscosity plots at relatively higher concentrations than the ones used for light scattering experiments show linearity (Figure 2). This may be a result of the shift of equilibrium completely in favor of the micelles and

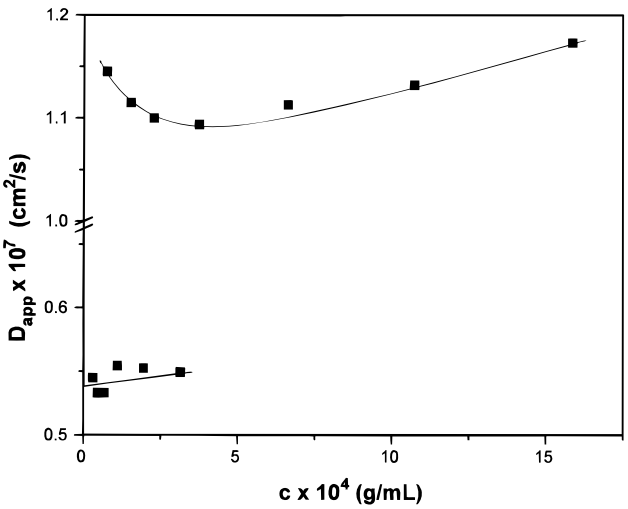

Figure 3. Apparent diffusion coefficient vs concentration for sample S_2IS_2 (top) and sample (S,I)I(I,S) (bottom) in *n*-decane at 25 °C.

to a constant number of chains, independent of concentration, per micelle. The $[\eta]$ values are smaller than the ones obtained in the good solvent. k_H values are found to be increased and very close to the theoretical value for hard spheres ($k_H = 0.99$[49]). However, the k_H calculated for the π copolymer is larger than the one determined for the H sample. The difference (about 20%) is outside the estimated experimental error (about 10%). Experimental R_v values are larger than the ones attributed to the unimer, supporting the static light scattering results for the presence of multimolecular aggregates in *n*-decane solutions.

The concentration dependence of D_{app} (Figure 3) is similar to the one found in static light scattering plots. The $D_{0,app}$ values are lower than the ones obtained in THF, reflecting the decreased mobility of the supramolecular structures in solution. The angular dependence of the diffusion coefficient is negligible. The second moment values, μ_2/Γ^2, are small (considerably lower than 0.1 at high concentrations), indicating low polydispersity of the micelles. The k_D values are increased in comparison to the THF solutions, despite the low A_2 values, due to the increase in the molecular weight during the association process ($k_D = 2A_2M + k_f - v$, where k_f is the coefficient of the concentration dependence of the friction coefficient and v is the partial specific volume of the polymer). The R_h values are also increased and are in good agreement with the R_v values. The R_v/R_h ratio is very close to unity (closer in the π copolymer case). Repetition of the experiment gave the same results. This latter result, in conjuction with the low $[\eta]$ values and the increased k_H values, indicates that the micelles of the graft copolymers, in *n*-decane, are very compact and behave in solution like hard spheres. The β_{MFS} values for the H and π copolymers, 2.27×10^6 and 2.09×10^6, respectively, point to the same conclusion.

Despite the fact that the difference (9%) of the β_{MFS} values is near the upper limit of estimated error (about 10%), duplication of the experiments allows us to conclude that the π copolymer seems to be more compact and seems to closely resemble hard spheres. This can be understood if we take into account the differences in architecture. The lengths of the insoluble branches (PS), which primarily determine the micellization behavior, are the same in each case. Also the lengths of the PI backbones are almost the same. However, the π

Table 3. Micellar Properties of Model Graft Copolymers in Ethyl Acetate at 25 °C for Sample S_2IS_2 and at 40 °C for Sample (S,I)I(I,S)

sample	$M_{w,app}$ $\times 10^{-6}$	A_2 $\times 10^6$	N_w[a]	$[\eta]$ (mL/g)	k_H	R_v (nm)	$D_{0,app}$ (cm^2/s) $\times 10^8$	k_D	R_h (nm)
S_2IS_2	9.13	0.47	52	25.3	0.24	33.2	0.46	9110	1126
(S,I)I(I,S)	2.16	−27	15	30.2	0.97	8.7	43.9	−18	13.2

[a] Degree of association. Note: Extrapolation of viscosity data at low concentrations for sample S_2IS_2 gives $[\eta] = 29.9$ mL/g, $k_H = -2.1$, and $R_v = 35.1$ nm. From the value of $D_{q=0}$ ($=3.31 \times 10^{-8}$ cm^2/s) for the highest concentration, $R_h = 155$ nm. The R_v value for sample (S,I)I(I,S) has been calculated from viscosity measurements by extrapolation at zero concentration, and the R_h value has been calculated using data above cmc.

copolymer has only two branches, equally spaced on the backbone, where the H copolymer has four branches located at the ends of the backbone. The experimental results point to the picture of spherelike micelles with polystyrene cores and poyisoprene coronas in *n*-decane for these polymers. In the case of the π copolymer, for each collapsed PS block there exist two PI blocks (one loose backbone end and half of the bridge), whereas for the H copolymer case, there is one half of the bridge for each pair of end branches. Taking into account the greater entropy penalty that the H's bridge has to pay in the looped configuration, in comparison to the π's smaller bridge, and the steric hindrance exercised by two neighboring collapsing branches, one must expect that the H copolymer should form less compact micelles. The same arguments can lead to the conclusion that micelles of the π copolymer can be stable even if they have lower aggregation numbers. Of course, in the present case the lower experimental aggregation number for the π-shaped copolymer can also be due to the lower PS content of this sample.

A comparison of the aggregation numbers for the model graft copolymer micelles with the ones observed for linear diblock copolymers of styrene and isoprene (or butadiene) in aliphatic solvents[5,6,8,10] (more or less similar systems with respect to thermodynamic interactions) shows that the model graft copolymers possess lower aggregation numbers. This may be attributed to the differences in topology. The influence of the topology can be viewed either as through the increase of steric hindrance of the soluble or insoluble blocks with increasing complexity of the architecture or through the solubilization effect of multiple soluble blocks connected to the insoluble ones (stabilization of micelles with lower aggregation numbers due to increased number of soluble blocks). As far as the triblock copolymer behavior is concerned, we cannot make any direct comparisons, since we could not find similar systems (molecular weight, composition, solvent, temperature) in the literature with which to compare. From the general trend of triblocks in solvents selective for the middle block, it seems that the π copolymer micelles have lower aggregation numbers but the ones formed by the H sample have comparable values of N_w.

C. Micellization in Ethyl Acetate. The behavior of the graft copolymers in ethyl acetate is more interesting. Micellar characteristics for the samples under investigation are given in Table 3. Static light scattering measurements (Figure 4) show that the H copolymer associates into micelles formed by 52 chains on average. The initial decrease of the reduced scattering intensity at low c is very steep, and the values for the apparent molecular weight of the micelles are almost constant for $2 \times 10^{-4} \leq c \leq 4.3 \times 10^{-3}$ g/mL. No cmc could be

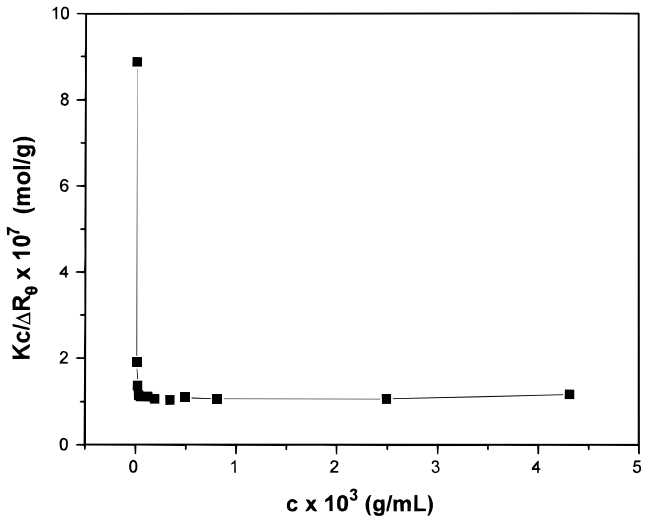

Figure 4. Static light scattering plot for sample S_2IS_2 in ethyl acetate at 25 °C.

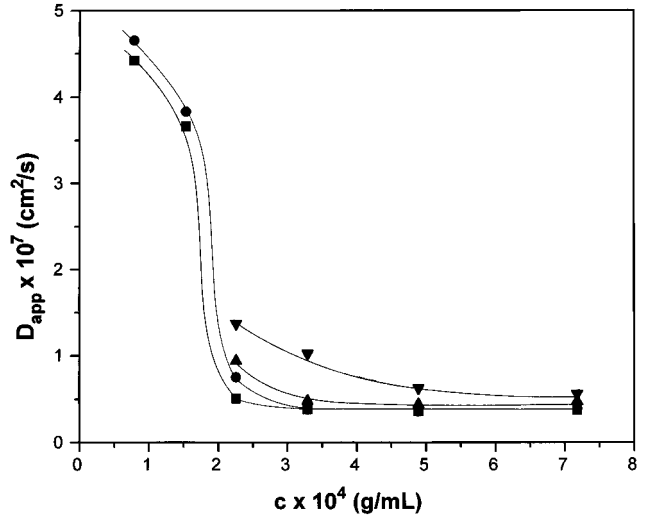

Figure 5. Apparent diffusion coefficient vs concentration for sample S_2IS_2 in ethyl acetate at 25 °C, at various angles (■) 37.5°; (●) 45°; (▲) 60°; (▼) 90°). For the first two lower concentrations, the light scattering intensity was very low in order to obtain a reasonable correlation function at angles higher than 45°. Notice the approach to angular independence of D_{app} at the highest concentration (see text for discussion).

detected for c as low as 6.5×10^{-6} g/mL. The A_2 value is very small. The dynamic light scattering data present a more complex picture (Figure 5). The change in slope in the concentration dependence of $D_{q=0,app}$ occurs in approximately the same range as for the static light scattering plots (Figure 5). The angular dependence of D_{app} is large in the transition region, becoming very small at the highest concentration studied (Figure 5). A parallel decrease of the second moment values by increasing concentration is also observed. Additionally, extrapolated values for $D_{0,app}$ from the high-concentration region are extremely small, leading to extremely large values for the R_h of the aggregates. The calculated k_D is also extremely large (Table 3). However, taking the D_{app} value at the highest concentration, where its angular dependence is negligible, a more realistic value of $R_h = 155$ nm is calculated. The viscosity data on the other hand (Figure 6) show an upturn at low concentrations and at $c > 4 \times 10^{-3}$ g/mL the k_H becomes positive. The extrapolated values of $[\eta]$ from different concentration regions are different but considerably smaller than

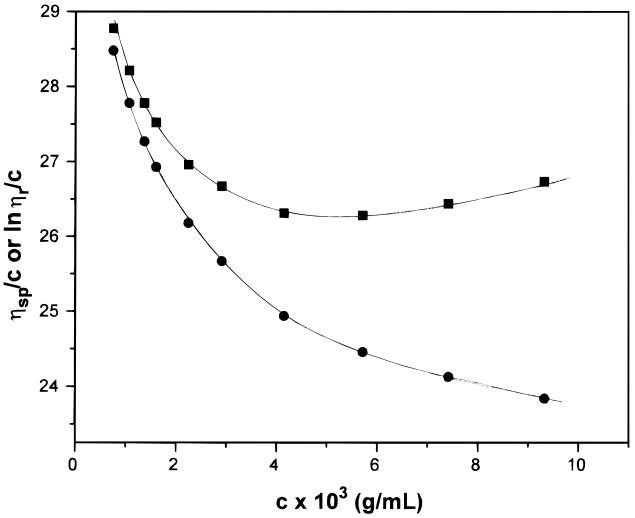

Figure 6. Viscosity plots for sample S_2IS_2 in ethyl acetate at 25 °C; (■) Huggins plot; (●) Kraemer plot. Notice the upturn at c lower than $\sim 4 \times 10^{-3}$ g/mL (see text for discussion).

the value determined in THF in any case. The calculated R_v is also smaller than the R_h determined by dynamic light scattering (Table 3). This may be a consequence of the different concentration range studied in the two methods (because of experimental accuracy and instrumental limitations in light scattering methods, the viscosity measurements cover a higher concentration region) and also their different sensitivities to the presence of supramolecular structures in solution. The increase in η_{sp}/c might also be attributed to the decrease in the micelle density ($[\eta] \propto 1/\rho_{micelle}$). It is also relevant to note that the concentration dependence of D_{app} at 90°, where the contribution of the larger particles is minimal, shows a negative slope (negative k_D indicates intermolecular attractive interactions), and the R_h calculated from the extrapolated value of D_{app} is equal to 31.8 nm (in better agreement with the viscosity data).

Taking into account the available data from the different methods, we can explain the behavior of H copolymer in ethyl acetate as follows. At c lower than $\sim 5 \times 10^{-4}$ g/mL, both unimers and multimers exist, with the equilibrium shifting in favor of the micelles as concentration increases. At c greater than 5×10^{-4} g/mL, micelles exist predominantly in solution as indicated from the constancy of $M_{w,app}$ values. However, the size (and maybe shape) of the aggregates still changes until $c \sim 4 \times 10^{-3}$ g/mL. In the low limit of this region, large and loose aggregates are formed since the micellar dimensions are large (although decreasing with increasing c) and the molecular weight remains constant, which tend to increase the viscosity of the solution (upturn in Figure 6). Dynamic light scattering results show that their polydispersity is large. No definite conclusions about the shape of these aggregates can be drawn with the data at hand. Their compactness and uniformity in size seem to increase with concentration (second moment values decrease and k_H becomes positive, taking a normal value for flexible polymers). The discrepancy in the R_h and R_v values may also indicate that the loose aggregates dissociate, to some extent, under shear. Large aggregates with loose structures near the cmc were also observed in other micelle-forming systems involving diblock and triblock copolymers.[5−8,16−18]

In one particular case, Price et al.[16] observed worm-like aggregates of a poly(styrene-*b*-butadiene-*b*-styrene) copolymer in ethyl acetate, using light scattering and electron microscopy (a more or less similar system to our case). However, in our experiments the transition through the "anomalous" region is relatively "smooth". Additionally, the H copolymer shows "anomalies" only with respect to the size and polydispersity of the aggregates, where Price et al. also observed increased aggregation numbers in the "anomalous" region. This statement is made under the assumption that our static light scattering measurements extend beyond the anomalous concentration region. The assumption is supported by the last data point of the DLS measurements, where the angular dependence of D_{app} is negligible and μ_2/Γ^2 values are equal to ~0.1 (indicating spherical micelles with relatively low polydispersity). From a different point of view, one can postulate that the system, on going from unimers to monodisperse micelles, in the classical sense passes through the intermediate formation of loosely bound aggregates, which are then transformed in the spherical monodisperse micelles, with no appreciable change in the aggregation number during this "transition". An analogous situation may also have been observed on the poly(styrene-*b*-isoprene-*b*-styrene) sample studied by Raspaud et al.[23] in heptane (although in this case the solvent is selective for the middle block). Whether this behavior depends on macromolecular architecture or not remains an open question.

Surely the solvent quality, with respect to the insoluble and maybe the soluble block, plays some role. From the solubility behavior of PS and PI homopolymers in *n*-decane and ethyl acetate, respectively, we conclude that *n*-decane is a much stronger precipitant for PS than ethyl acetate is for PI. From this result alone one would expect that micelles with a PS core in *n*-decane should be more compact than micelles with PI cores in ethyl acetate, since greater swelling is allowed in the latter case. Furthermore, ethyl acetate seems to be a good solvent for PS whereas *n*-decane is a marginal solvent for PI (solubility parameter values,[50] δ: for PS, $\delta = 8.6-10.3$ $(cal/cm^3)^{1/2}$; for PI, $\delta = 7.4-8.4$ $(cal/cm^3)^{1/2}$; for *n*-decane, $\delta = 6.6$ $(cal/cm^3)^{1/2}$; for ethyl acetate, $\delta = 9.1$ $(cal/cm^3)^{1/2}$). Finally, comparison of the aggregation number for the H copolymer with the ones found for the sample studied by Price et al. shows that the H copolymer forms micelles with a smaller average number of chains, despite its higher PS content and molecular weight, probably due to the larger number of soluble blocks per molecule (four instead of two for a triblock copolymer).

The situation is somewhat different for the π copolymer. LALLS measurements show that the molecular weight of the solute remains constant ($M_{w,app} = 137\,000$), and equal to that of the unimer (Table 1) for concentrations up to $c = 2 \times 10^{-3}$ g/mL (Figure 7). The A_2 has a lower value than in THF, a result that reflects the reduced thermodynamic quality of the solvent. For concentrations larger than 2×10^{-3} g/mL, the reduced scattering intensity decreases steeply, indicating the presence of a cmc at this concentration range. The molecular weight calculated from the high-concentration range corresponds to micelles containing 15 chains on average. In this region, although only three solutions have been studied due to the limited amount of the sample, it seems the second virial coefficient is negative, meaning that the equilibrium is not completely shifted in favor of the micelles. The dependence of the diffusion coefficient on concentration (Figure 8) is linear for $c < 2 \times 10^{-3}$ g/mL and k_D is negative ($k_D = -58$). The R_h

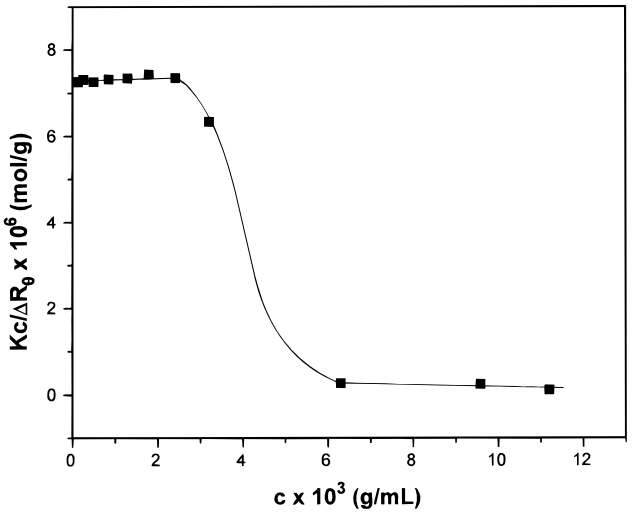

Figure 7. Static light scattering plots for sample (S,I)I(I,S) in ethyl acetate at 40 °C ($\theta = 4.8°$).

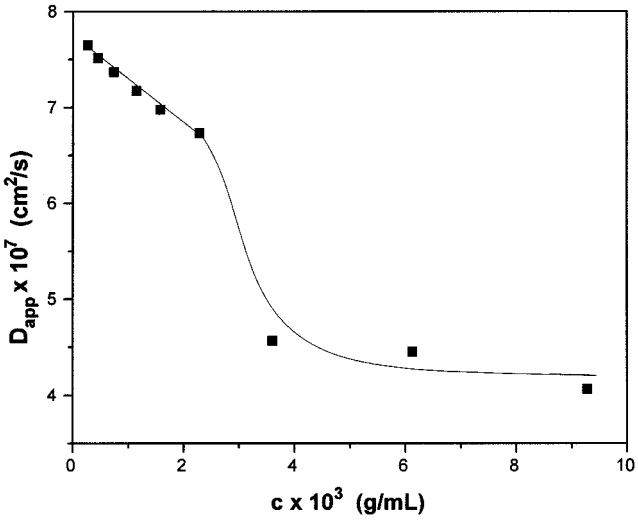

Figure 8. Apparent diffusion coefficient vs concentration for sample (S,I)I(I,S) in ethyl acetate at 40 °C.

calculated from the extrapolated D_0 value is smaller than the one found in THF and equal to 8.4 nm. A cmc is evident also in this plot at almost the same concentration with the static light scattering measurements. At the high-concentration region the experimental values are shown in Table 3. The negative k_D is consistent with the negative A_2 value. Similarly, the $[\eta]$ value is lower than in THF but the k_H value is close to the theoretical prediction for hard spheres. The calculated R_v is lower than the one in THF and close to the R_h value determined by dynamic light scattering by extrapolation to zero concentration from the low-concentration region. The ratio $R_v/R_h = 1.04$ is very close to the theoretical value for hard spheres, indicating the compactness of the unimolecular micelles. These experimental facts point to the conclusion that the copolymer forms monomolecular micelles in ethyl acetate at concentrations lower than 2×10^{-3} g/mL. Multimolecular micelles with a more or less spherelike structure are present at higher concentrations. The micellization behavior is more consistent with a closed association model. The relatively low aggregation number and the presence of a cmc at high concentrations, compared with the SBS sample studied by Price et al., can be attributed to the differences in macromolecular architecture, which produces additional constraints in the organization of the chains in multimolecular micelles.

Conclusions

The two well-defined graft copolymers of styrene and isoprene of the H and π architecture form multimolecular micelles in *n*-decane, a selective solvent for the polyisoprene backbones. The aggregation numbers of both copolymers were found to be lower than the ones determined for similar systems of diblock and triblock copolymers in selective solvents. Analysis of the hydrodynamic properties shows that their micelles behave like hard spheres, the similarity being greater for the π copolymer micelles. In ethyl acetate, a selective solvent for the polystyrene branches, multimolecular micelles are also present. In the H copolymer solutions, the formation of multimolecular micelles is accomplished through the transient formation of large, loosely bound aggregates above the critical micelle concentration. In the π copolymer case, the whole concentration region, from the existence of unimolecular micelles to the formation of multimolecular micelles, was observed, indicating that its micellization behavior can be described by the closed association model. The influence of the macromolecular architecture on the micellization behavior can be described mainly through the lower aggregation numbers, due to the additional constraints imposed to the organization of complex macromolecular chains in a micelle containing many unimers and to the presence of an increased number of soluble blocks per insoluble one.

Acknowledgment. S.P. and J.W.M. gratefully aknowledge the financial support of the U.S. Army Research Office for the research conducted at UAB (Grant DAAH04-94-G-0245). The technical assistance of Mr. Yunan Wan is greatly appreciated. We also thank the two Referees for their helpful criticisms of the original manuscript.

References and Notes

(1) Elias, H.-G. *Int. J. Polym. Mater.* **1976**, *4*, 209.
(2) Riess, G.; Hurtrez, G.; Bahadur, P. In *Encyclopedia of Polymer Science and Engineering*, 2nd ed.; Mark, H. F., Bikales, N. M., Overberger, C. G., Menges, G., Eds, Wiley: New York, 1985; Vol. 2, pp 324−436.
(3) (a) Merrett, F. M. *J. Polym. Sci.* **1957**, *24*, 467. (b) Molau, G. E.; Wittbrodt, W. M. *Macromolecules* **1968**, *1*, 260.
(4) Tuzar, Z.; Kratochvil, P. *Surf. Colloid Sci.* **1993**, *15*, 1.
(5) Tsunashima, Y.; Hirata, M.; Kawamata, Y. *Macromolecules* **1990**, *23*, 1089.
(6) Tsunashima, Y. *Macromolecules* **1990**, *23*, 2963.
(7) Sikora, A.; Tuzar, Z. *Makromol. Chem.* **1983**, *184*, 2049.
(8) Mandema, W.; Zeldenrust, H.; Emeis, C. A. *Makromol. Chem.* **1979**, *180*, 1521.
(9) Stejskal, J.; Hlavata, D.; Sikora, A.; Konak, C.; Plestil, J.; Kratochvil, P. *Polymer* **1992**, *33*, 3675.
(10) Bahadur, P.; Sastry, N. V.; Marti, S.; Riess, G. *Colloids Surf.* **1985**, *16*, 337.
(11) Price, C.; McAdam, J. D. G.; Lally, T. P.; Woods, D. *Polymer* **1974**, *15*, 228.
(12) Hilfiker, R.; Chu, B.; Xu, Z. J. *Colloid Interface Sci.* **1989**, *133*, 176.
(13) Noolandi, J.; Hong, K. M. *Macromolecules* **1983**, *16*, 1443.
(14) Halperin, A. *Macromolecules* **1987**, *20*, 2943.
(15) Nagarajan, R.; Ganesh, K. *J. Chem. Phys.* **1989**, *90*, 5843.
(16) Canham, P. A.; Lally, T. P.; Price, C.; Stubberfield, R. B. *J. Chem. Soc., Faraday Trans. 1* **1980**, *70*, 1857.
(17) Bednar, B.; Devaty, J.; Koupalova, B.; Kralicek, J.; Tuzar, Z. *Polymer* **1984**, *25*, 1178.
(18) Tuzar, Z.; Stepanek, P.; Konak, C.; Kratochvil, P. *J. Colloid Interface Sci.* **1985**, *105*, 372.
(19) (a) Tuzar, Z.; Kratochvil, P. *Makromol. Chem.* **1972**, *160*, 301. (b) Plestil, J.; Baldrian, J. *Makromol. Chem.* **1973**, *174*, 183.

(20) Tuzar, Z.; Petrus, V.; Kratochvil, P. *Makromol. Chem.* **1974**, *175*, 3181.
(21) Tuzar, Z.; Plestil, J.; Konak, C.; Hlavata, D.; Sikora, A. *Makromol. Chem.* **1983**, *184*, 2111.
(22) Tuzar, Z.; Konak, C.; Stepanek, P.; Plestil, J.; Kratochvil, P.; Prochazka, K. *Polymer* **1990**, *31*, 2118.
(23) Raspaud, E.; Lairez, D.; Adam, M.; Carton, J.-P. *Macromolecules* **1994**, *27*, 2956.
(24) Villacampa, M.; Quintana, J. R.; Salazar, R.; Katime, I. *Macromolecules* **1995**, *28*, 1025.
(25) Balsara, N. P.; Tirrell, M.; Lodge, T. P. *Macromolecules* **1991**, *24*, 1975.
(26) Prochazka, O.; Tuzar, Z.; Kratochvil, P. *Polymer* **1991**, *32*, 3038.
(27) ten Brinke, G.; Hadziioannou, G. *Macromolecules* **1987**, *20*, 486.
(28) Price, C.; Woods, D. *Polymer* **1974**, *15*, 389.
(29) Candau, S.; Boutillier, J.; Candau, F. *Polymer* **1979**, *20*, 1237.
(30) Candau, S.; Guenet, J.-M.; Boutillier, J.; Picot, C. *Polymer* **1979**, *20*, 1227.
(31) Selb, J.; Gallot, Y. *Makromol. Chem.* **1981**, *182*, 1775.
(32) Tuzar, Z.; Kratochvil, P.; Prochazka, K.; Contractor, K.; Hadjichristidis, N. *Makromol. Chem.* **1989**, *190*, 2967.
(33) Prochazka, K.; Glockner, G.; Hoff, M.; Tuzar, Z. *Makromol. Chem.* **1984**, *185*, 1187.
(34) Bayer, U.; Stadler, R. *Macromol. Chem. Phys.* **1994**, *195*, 2709.
(35) Tsitsilianis, C.; Papanagopoulos, D.; Lutz, P. *Polymer* **1995**, *36*, 3745.
(36) Iatrou, H.; Willner, L.; Hadjichristidis, N.; Halperin, A.; Richter, D. *Macromolecules* **1996**, *29*, 581.
(37) Morton, M.; Fetters, L. J. *Rubber Chem. Technol.* **1975**, *48*, 359.
(38) Pochan, D.; Gido, S. P.; Pispas, S.; Mays, J. W.; Hadjichristidis, N. *Macromolecules*, in press.
(39) Yamakawa, H. *Modern Theory of Polymer Solutions*; Harper and Row: New York, 1971.
(40) Roovers, J.; Martin, J. E. *J. Polym. Sci., Polym. Phys. Ed.* **1989**, *27*, 2513.
(41) Roovers, J.; Toporowski, P. M. *J. Polym. Sci., Polym. Phys. Ed.* **1980**, *18*, 1907.
(42) Davidson, N. S.; Fetters, L. J.; Funk, W. G.; Hadjichristidis, N.; Graessley, W. W. *Macromolecules* **1987**, *20*, 2614.
(43) Lindner, J. S.; Wilson, W. W.; Mays, J. W. *Macromolecules* **1988**, *21*, 3304.
(44) Lewis, M. E.; Nan, S.; Mays, J. W. *Macromolecules* **1991**, *24*, 197, 4857.
(45) Fetters, L. J.; Hadjichristidis, N.; Lindner, J. S.; Mays, J. W.; Wilson, W. W. *Macromolecules* **1991**, *24*, 3127.
(46) Allorio, S.; Pispas, S.; Siakali-Kioulafa, E.; Hadjichristidis, N. *J. Polym. Sci., Part B: Polym. Phys.* **1995**, *33*, 2229.
(47) a) Mandelkern, L.; Flory, P. J. *J. Chem. Phys.* **1952**, *20*, 212. (b) Scheraga, H. A.; Mandelkern, L. *J. Am. Chem. Soc.* **1953**, *175*, 3181.
(48) Elias, H.-G. In *Light Scattering from Polymer Solutions*; Huglin, M., Ed., Academic Press: London, 1972: Chapter 9.
(49) Batchelor, G. K. *J. Fluid Mech.* **1977**, *83*, 97.
(50) Brandrup, J.; Immergut, E. H., Eds. *Polymer Handbook*, 2nd ed.; John Wiley & Sons, Inc.: New York, 1975.

MA960474B